Chemical Science

EDGE ARTICLE

Selective photocatalytic aerobic bromination with hydrogen bromide *via* an electron-transfer state of 9-mesityl-10-methylacridinium ion†

Kei Ohkubo,[a] Kentaro Mizushima,[a] Ryosuke Iwata[a] and Shunichi Fukuzumi[*ab]

Photocatalytic bromination of aromatic hydrocarbons by molecular oxygen with hydrogen bromide occurs efficiently to produce monobrominated products selectively using 9-mesityl-10-methylacridinium ion (Acr^+–Mes) as a photocatalyst under visible light irradiation. Both the product yield and selectivity for the bromination of 1,3,5-trimethoxybenzene were 100% with a quantum yield of 4.8%. The photocatalytic turnover number is 900 based on the initial concentration of Acr^+–Mes. The reactive radical intermediates involved in the photocatalytic cycle have been successfully detected by laser flash photolysis measurements. The photocatalytic bromination is initiated by photoinduced electron transfer from the mesitylene moiety to the singlet excited state of acridinium ion, which results in formation of the electron-transfer state of Acr^+–Mes ($Acr^{\bullet}$–Mes$^{\bullet+}$), followed by electron transfer from aromatic hydrocarbons to the mesitylene radical cation moiety and electron transfer from the acridinyl radical moiety to O_2. The resulting radical cations of aromatic hydrocarbons react with Br^- to produce the corresponding monobrominated products selectively.

Introduction

Halogenated organic compounds provide very important synthetic intermediates in organic synthesis for many applications in the fields of material science, chemical industry and medicine.[1] Bromination of arenes has been one of the most important and fundamental reactions in organic synthesis, providing key precursors for various transformations such as Grignard reactions and Suzuki–Miyaura coupling.[1] A number of protocols are available to achieve bromination with elemental bromine and *N*-bromosuccinimide (NBS), however, they are toxic, hazardous and less selective.[2] Extensive efforts have been made to develop an environmentally friendly bromo source that can be used under mild conditions.[2–17] Molecular bromine is most frequently used for bromination of organic compounds. To avoid the use of molecular bromine, NBS has been used for bromination, however, molecular bromine is used to prepare NBS. Alternatively, the brominating reagent can be generated by the oxidation of bromide ion where hydrogen peroxide has frequently been used as a green oxidant that produces only water as the side product.[2–6] The better oxidant is obviously oxygen. On the other hand, radical cations are known to react with

a nucleophile to form various adducts.[5,6,16,17] Electrophilic addition of Br^- to radical cations would enable selective bromination following electron transfer. However, there has been no report on selective bromination of organic compounds *via* the electron-transfer oxidation using oxygen as an oxidant.[18,19]

We report herein that 9-mesityl-10-methylacridinium perchlorate (Acr^+–Mes)[20] acts as an efficient photocatalyst for selective bromination of aromatic hydrocarbons and thiophenes with aqueous HBr as a Br source and O_2 as an oxidant under visible light irradiation. The electron-transfer state, $Acr^{\bullet}$–Mes$^{\bullet+}$, produced upon photoexcitation of Acr^+–Mes, has both strong oxidizing and reducing ability, and this enables not only oxidation of alkyl aromatic compounds and thiophenes but also reduction of O_2.[20–22] The photocatalytic mechanism is clarified by detecting radical intermediates involved in the photocatalytic reactions with use of laser flash photolysis. The present study provides a unique bromination pathway of aromatic hydrocarbons and thiophenes with HBr as a Br source and oxygen as a green oxidant without using a toxic bromine source. It should be noted that bromination of thiophenes is particularly important in the preparation of oligothiophenes and polythiophenes,[23–25] which have many applications as conductive, semiconductive, nonlinear optical and liquid crystalline materials.[26]

Results and discussion

### Photocatalytic bromination of trimethoxybenzene with O_2

Visible light irradiation of $(Acr^+–Mes)ClO_4^-$ (λ_{max} = 430 nm, 0.20 mM) in O_2-saturated acetonitrile (MeCN) containing

[a] Department of Material and Life Science, Graduate School of Engineering, Osaka University, 2-1 Yamada-oka, Suita, Osaka, 565-0871, Japan. E-mail: fukuzumi@chem.eng.osaka-u.ac.jp; Fax: +81-6-6879-7370
[b] Department of Bioinspired Chemistry (WCU), Ewha Womans University, Seoul, 120-750, Korea
† Electronic supplementary information (ESI) available: ^{1}H NMR chemical shift of products (S1) and time course in bromination of TMB. See DOI: 10.1039/c0sc00535e

1,2,4-trimethoxybenzene (TMB, 4.0 mM) and 50% aqueous HBr ([HBr] = 20 mM, [H$_2$O] = 100 mM) with a xenon lamp attached with a cut-off filter (λ < 320 nm) for 20 min resulted in formation of a brominated product, 2,4,5-trimethoxy-bromobenzene. The bromination was monitored by ^{1}H NMR as shown in Fig. 1. The product was identified and quantified by comparison of the spectra with that of authentic sample. The time profiles conversion of TMB and formation of the corresponding monobrominated product are the same in the photocatalytic reaction (see the supplementary information (ESI) S1†). The overall stoichiometry of the photocatalytic reaction is given by eqn (1).

$$(1)$$
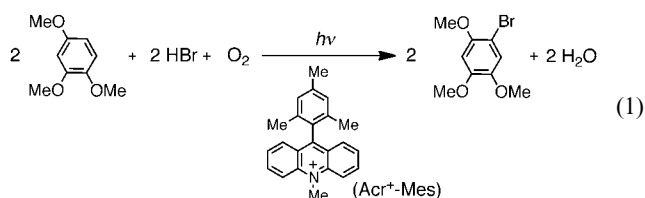
Both the yield and selectivity of the monobrominated product, 2,4,5-trimethoxybromobenzene are 100%, because no further brominated product, dibromo- or tribromo-derivative, was produced as shown in ^{1}H NMR spectra (Fig. 1c). The products and quantum yields were determined by ^{1}H NMR and GC-MS spectroscopies (see the experimental section), which are also listed in Table 1. We have also confirmed that no decomposition of Acr$^+$–Mes occured after the photocatalytic reaction as there was no disappearance of the ^{1}H NMR signal due to Acr$^+$–Mes in Fig. 1.
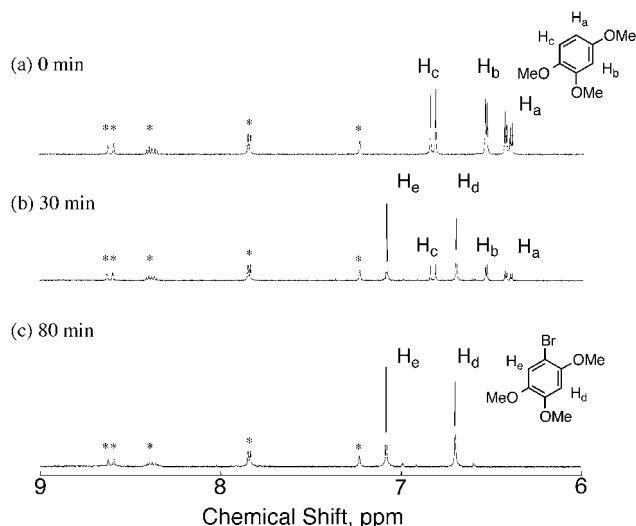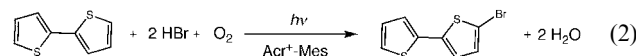
Photocatalytic bromination reactions of various aromatic compounds were also examined under the same conditions (Table 1). The efficient catalytic bromination reactions were observed in the case of the methoxy-substituted benzenes. A preparative scale photocatalytic reaction of TMB (200 mg, 1.2

mmol) with 50% aqueous HBr (160 μL 1.5 mmol) in the presence of Acr$^+$–Mes (0.044 mmol) in oxygen-saturated MeCN (100 mL) under photoirradiation by a xenon lamp for 24 h afforded the brominated product in 100% selectivity and in 81% yield (NMR criterion; 61% isolated yield). The isolation procedure is described in the Experimental Section.

When methoxy-substituted aromatic compounds were replaced by toluene derivatives (entries 9, 10 in Table 1), the consumption of substrate occurred efficiently under the same experimental conditions. However, the yield of bromo product and selectivity were significantly lower as compared with methoxy-substituted benzenes, photobromination competes with photooxygenation with oxygen to yield the corresponding aromatic aldehyde.

Photocatalytic bromination of thiophene

Photocatalytic bromination reactions of 3-methylthiophene, bithiophene and trithiophene also occur efficiently with Acr$^+$–Mes and HBr. Visible light irradiation of the absorption band of Acr$^+$–Mes (0.20 mM) in an O$_2$-saturated MeCN solution containing dithiophene (4.0 mM) and HBr (20 mM) for 2 h by xenon lamp results in the selective formation of a monobrominated product [eqn (2)]. No further brominated product, 2,2′-dibromobithiophene was observed under the present experimental conditions. The selective monobromination of 3-methylthiophene also occurred to yield 2-bromo-3-methylthiophene. In contrast to the case of trithiophene, the monobromo product is initially formed together with the small amount of dibromo product. When the starting material was consumed after the photoirradiation for 1.5 h, the yields of mono- and dibromo products are 50% and 50%, respectively. The summary of photobromination of thiophene derivatives is listed in Table 2.
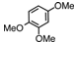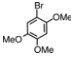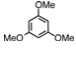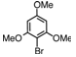

$$(2)$$

Mechanism of photocatalytic bromination of substrates with Acr$^+$–Mes, HBr and O$_2$

The photodynamics of the photocatalytic bromination of TMB with Acr$^+$–Mes, HBr and O$_2$ was examined by nanosecond laser flash photolysis. A transient absorption spectrum observed after the laser pulse excitation at 430 nm of an MeCN solution of Acr$^+$–Mes is assigned to the electron-transfer state of Acr$^+$–Mes (Acr$^•$–Mes$^{•+}$: λ_{max} = 500 nm) produced by intramolecular electron transfer from the mesitylene (Mes) moiety to the singlet excited state of acridinium (Acr$^+$) moiety (Fig. 2, blue).[20] The broad absorption band in the near IR region (800–1100 nm) is attributed to the π-dimer of Acr$^•$–Mes$^{•+}$ with the ground state of Acr$^+$–Mes.[27,28] In the presence of TMB, a new band at 450 nm appeared at 12 μs, which is assigned to the TMB radical cation (TMB$^{•+}$)[29] in Fig. 2. The rise time profile for formation of TMB$^{•+}$ is monitored at 450 nm as shown in Fig. 3a, which obeys pseudo-first-order kinetics. The rate constant for formation of TMB$^{•+}$ (k_{rise}) increases linearly with increasing concentration of TMB. The second-order rate constant of electron transfer from TMB to the Mes$^{•+}$ of the electron-transfer (ET) state of Acr$^+$–Mes was

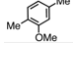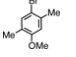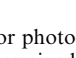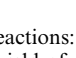**Fig. 1** ^{1}H NMR spectra of an oxygen-saturated CD$_3$CN solution containing [Acr$^+$–Mes]ClO$_4^-$ (2.0 × 10^{-4} M), 1,2,4-trimethoxybenzene (TMB) (4.0 × 10^{-3} M) and HBr (2.0 × 10^{-2} M) (a) before and after photoirradiation [(b) 30 min and (c) 80 min, λ > 320 nm]. Asterisks denote the peaks due to (Acr$^+$–Mes)ClO$_4^-$.

Table 1 Product and quantum yields for photocatalytic bromination of methoxy-substituted aromatic compounds by O_2 and HBr with Acr⁺–Mes in MeCN and one-electron oxidation potentials of substrates (E_{ox})

Entry	Substrate	Product	Conversion,[a]%	Yield,[a]%	Time, h	Quantum yield,[b]%	E_{ox},[c] V
1	(structure)	(structure)	>99	>99	0.3	4.3	0.96
2	(structure)	(structure)	>99	>99	0.3	4.8	1.43
3	(structure)	(structure)	>99	>99	0.3	3.9	1.49
4	(structure)	(structure)	>99	>99	0.5	3.1	1.34
5	(structure)	(structure)	>99	>99	1.5	1.1	1.42
6	(structure)	(structure)	>99	>99	2	0.26	1.47
7	(structure)	(structure)	>99	>99	16	0.01	1.76
8	(structure)	(structure)	>99	78[d]	3	0.10	1.45
9	(structure)	(structure)	>99	53	2	0.36	1.33
10	(structure)	(structure)	>99	44	2	0.32	1.47
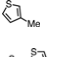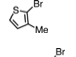
[a] Conditions for photochemical reactions: [substrate] = 4.0 mM; [Acr⁺–Mes ClO₄⁻] = 0.20 mM; [HBr] = 20 mM; [H₂O] = 100 mM. [b] The quantum yields were determined from the yield of monobrominated product. Experimental error within 0.03%. [c] Values (*versus* SCE) are determined by CV and second harmonic ac voltammetry (SHACV). [d] Minor product is the dibromo compounds.

determined from the slope of the linear plot of k_{rise} versus [TMB] to be $k_{TMB} = 2.0 \times 10^{10}$ M⁻¹ s⁻¹ (Fig. 3b). The absorption band of TMB˙⁺ disappeared with second-order kinetics *via* back electron transfer from the Acr˙ moiety of the ET state to TMB˙⁺ (Fig. 4a). The decay of TMB˙⁺ was accelerated by addition of HBr. The decay time profile obeys first-order kinetics in the presence of HBr. The observed decay rate constant (k_{decay}) increases linearly with increasing concentrations of HBr as shown in Fig. 4b. Thus, TMB˙⁺ efficiently reacts with Br⁻ to form the Br adduct radical [TMB(Br)˙]. The rate constant for the addition of Br⁻ was determined from the slope of k_{decay} versus [HBr] to be $k_{HBr} = 1.4 \times 10^8$ M⁻¹ s⁻¹ (Fig. 4b). The electron-transfer oxidation of Br⁻ in the photocatalytic reaction was also examined by quenching of Acr˙–Mes˙⁺ by HBr. The quenching rate constant of Acr˙–Mes˙⁺ with HBr is two orders of magnitude smaller (2.9×10^8 M⁻¹ s⁻¹) than the k_{TMB} value (Fig. 3b). Thus, the substrate (4.0 mM) rather than Br⁻ (20 mM) is preferentially oxidized under the present experimental conditions.[30]

The one-electron oxidation potentials (E_{ox}) of aromatic compounds in deaerated MeCN are listed in Table 1. The E_{ox} values (0.96–1.76 V) are lower than the one-electron reduction potential of the ET state of Acr⁺–Mes (Acr˙–Mes˙⁺; $E_{red} = 2.06$ V *versus* SCE in MeCN).[21] Thus, electron transfer from an aromatic compound such as TMB to Acr˙–Mes˙⁺ is energetically favorable, whereas electron transfer from toluene ($E_{ox} = 2.20$ V)[31] and benzene (2.32 V)[31] to the Mes˙⁺ moiety is energetically unfavorable. Thus, no photocatalytic bromination of benzene or toluene occurs under the present experimental conditions. The decreased reactivity of methoxybenzene (entry 7 in Table 1) is attributed to the high E_{ox} value (1.76 V). On the

Table 2 Product and quantum yields for photocatalytic bromination of thiophenes by O_2 and HBr with Acr⁺–Mes in MeCN and one-electron oxidation potentials of thiophenes (E_{ox})

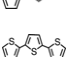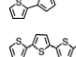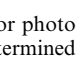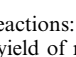| Entry	Thiophene	Product	Conversion,[a]%	Yield,[a]%	Time, h	Quantum yield,[b]%	E_{ox},[c] V
1	(structure)	(structure)	>99	81	2	0.38	1.67
2	(structure)	(structure)	>99	>99	1	1.3	1.23
3	(structure)	(structure)	>99	50[d]	1.5	0.96	0.97

[a] Conditions for photochemical reactions: [substrate] = 4.0 mM; [Acr⁺–Mes ClO₄⁻] = 0.20 mM; [HBr] = 20 mM; [H₂O] = 100 mM. [b] The quantum yields were determined from the yield of monobrominated product. Experimental error within 0.03%. [c] Values (*versus* SCE) are determined by CV and second harmonic ac voltammetry (SHACV). [d] The yield of dibromo product was 50%.
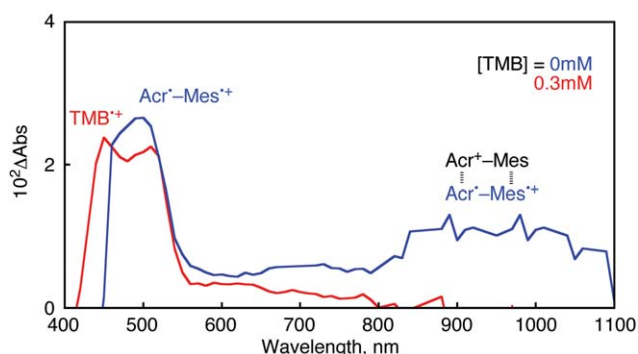
Fig. 2 Transient absorption spectra of the ET state of Acr$^+$–Mes (0.2 mM) in the absence and presence of TMB (0.3 mM) in deaerated MeCN after nanosecond laser excitation at 430 nm.
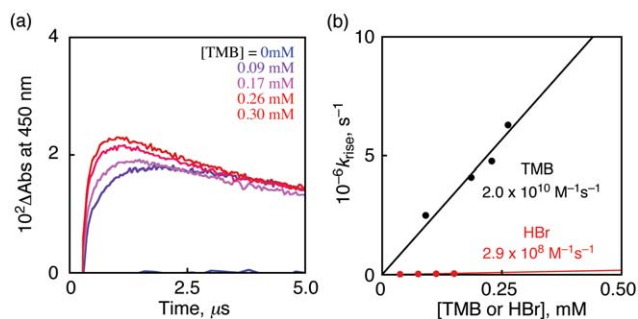
Fig. 3 (a) Transient absorbance time profiles at 450 nm due to TMB$^{\bullet+}$ for electron transfer from TMB (0–0.30 mM) to Acr$^{\bullet}$–Mes$^{\bullet+}$ in MeCN after nanosecond laser flash photolysis (λ_{ex} = 430 nm); (b) plot of k_{rise} versus [TMB] or [HBr] for the reaction of Acr$^{\bullet}$–Mes$^{\bullet+}$ with TMB or HBr.
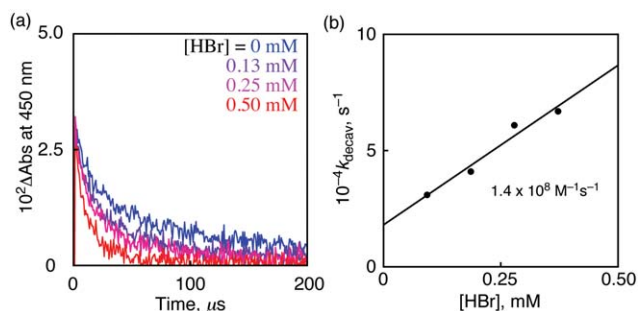
Fig. 4 (a) Transient absorbance time profiles at 450 nm due to TMB$^{\bullet+}$ in the absence and presence of HBr (0–0.50 mM) in O$_2$-saturated MeCN containing Acr$^+$–Mes (0.2 mM) after nanosecond laser flash photolysis (λ_{ex} = 430 nm); (b) plot of k_{decay} versus [HBr] for the reaction of TMB$^{\bullet+}$ with HBr.

other hand, the one-electron reduction of O$_2$ by the ET state of Acr$^+$–Mes in the presence of an acid is known to occur efficiently, producing HO$_2$$^{\bullet}$.[32] The rate constant of electron-transfer reduction of O$_2$ (k_{O_2}) has been reported to be 6.8 × 10^8 M^{-1} s^{-1}.[21]

The photocatalytic reaction is initiated by intramolecular photoinduced electron transfer from the Mes moiety to the singlet excited state of the Acr$^+$ moiety of Acr$^+$–Mes to generate Acr$^{\bullet}$– Mes$^{\bullet+}$ as shown in Scheme 1. The Mes$^{\bullet+}$ moiety can oxidize TMB to produce TMB$^{\bullet+}$, whereas the Acr$^{\bullet}$ moiety can reduce O$_2$

Scheme 1 Proposed photocatalytic reaction mechanism.

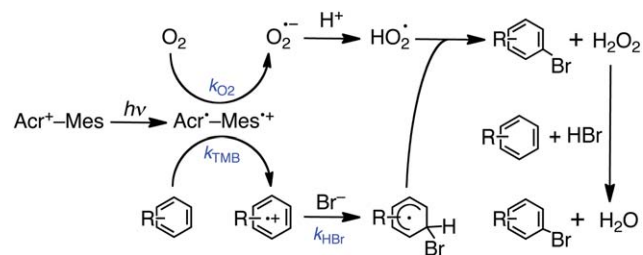to HO$_2$$^{\bullet}$. The TMB$^{\bullet+}$ produced reacts with Br$^-$ to form the Br adduct radical, which undergoes dehydrogenation with HO$_2$$^{\bullet}$ to afford the corresponding brominated product and hydrogen peroxide. Hydrogen peroxide further reacts with HBr and the substrate to produce another brominated product and H$_2$O.[33,34]

The quantum yield of photocatalytic bromination of TMB with Acr$^+$–Mes and HBr remains constant (4.3%) with increasing the concentration of TMB and the light intensity under the present experimental conditions (see Fig. 5). This suggests that no radical chain process is involved in the present photocatalytic aerobic bromination of substrates with HBr.

Selectivity of photocatalytic bromination

The selectivity of monobromination is controlled by the difference between the electron-transfer oxidation reactivity of brominated and unbrominated benzenes with the Mes$^{\bullet+}$ moiety of the ET state and also by the reactivity of the radical cations with Br$^-$. The one-electron oxidation potential of bromobenzene is lower than that of the benzene.[35] Thus, the electron-transfer oxidation reactions of brominated benzenes with the Mes$^{\bullet+}$ moiety of the ET state may be as efficient as those of unbrominated benzenes. Thus, the lower reactivity of brominated benzenes as compared with unbrominated benzenes in Table 1 may result from the lower reactivity of the radical cations of brominated benzenes. The atomic charges of the neutral and the radical cation of TMB are shown in Fig. 6, which are estimated by DFT calculations using the B3LYP/6-31+G(d,p) basis set. The position of the largest positive charge on the neutral aromatic compound is the same as that of the radical cation. This indicates that the nucleophilic bromination of the photo-generated radical cation species with Br$^-$ results in the same regioselectivity as that for the ordinary electrophilic bromination.

The determining steps of quantum yield for the bromination are electron-transfer oxidation of the substrate and electron-transfer reduction of O$_2$ with the ET state of Acr$^+$–Mes. The quantum yield of photobromination depends on the electron-transfer oxidation reactivity of substrates with the Mes$^{\bullet+}$ moiety and the reactivity of the radical cation with Br$^-$. The aromatic compounds without electron-donating substituent(s) have high oxidation potentials to afford the poor reactivity of electron-transfer oxidation. The higher is the E_{ox} value of substrate, the slower is electron-transfer rate, resulting in the lower quantum yield as shown in Table 1. The significant difference in the reactivity between 1,2,3- and 1,3,5-trimethoxybenzenes despite virtually the same E_{ox} values may result from the energy difference between the radical cation and brominated neutral radical,
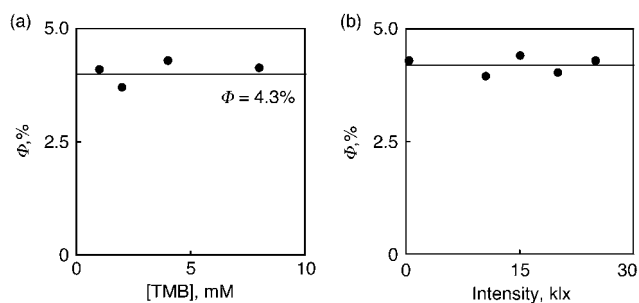
Fig. 5 (a) Dependence of the quantum yields (Φ) on [TMB] for photocatalytic bromination of TMB with Acr$^+$–Mes (0.2 mM) and HBr (4.0 mM) in O$_2$-saturated CD$_3$CN. Light intensity: 0.38 klx. (b) Dependence of the quantum yields (Φ) on excitation light intensity for photobromination of TMB (4.0 mM) with Acr$^+$–Mes (0.2 mM) and HBr (4.0 mM) in oxygen-saturated CD$_3$CN. Excitation wavelength: $\lambda = 430$ nm.
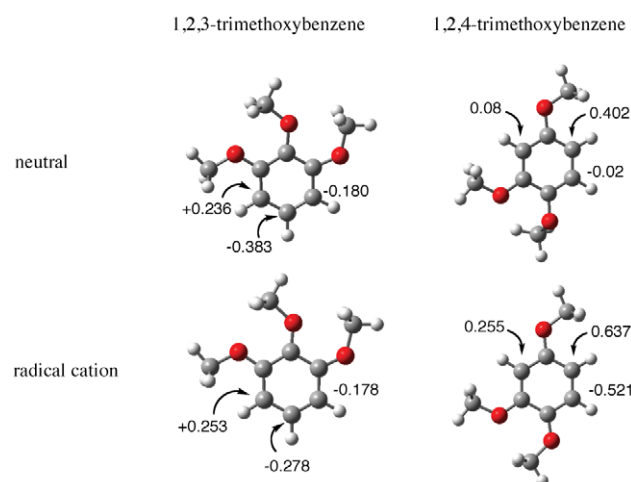
Fig. 6 Atomic charges on carbon atoms of 1,2,3- and 1,2,4-trimethoxybenzene of the neutral and radical cation forms calculated at the B3LYP/6-31+G(d,p) basis set.

which are estimated by DFT calculations at the B3LYP/6-31G(d) basis set (Table 3). The Br$^-$ adduct of the radical cation of 1,3,5-trimethoxybenzene is 8.5 kcal mol^{-1} more stable than that of 1,2,3-trimethoxybenzene.

When Acr$^+$–Mes was replaced by 9-mesityl-2,7,10-trimethyl-lacridinium ion (Me$_2$Acr$^+$–Mes)[21] as a photocatalyst which has a stronger reducing ability at the ET state ($E_{ox} = -0.67$ V versus

Table 3 Energies (in hartree) of the substrate radical cation and Br adduct radical and energy differences for the bromination of trimethoxybenzenes[a]

Substrate	Radical cation	Br adduct radical	Energy difference[b]
1,2,3-Trimethoxy-benzene	-575.5437207	-3147.5041129	8.5 kcal mol^{-1}
1,3,5-Trimethoxy-benzene	-575.550096	-3147.504112	0

[a] Calculated at the B3LYP/6-31G(d) basis set. [b] Normalized to -2571.9540161 hartree.

SCE) compared to Acr$^+$–Mes, the photocatalytic reaction rate of photobromination of TMB was slower than that with Acr$^+$–Mes. The yield of bromination of TMB was 38% with 37% consumption of substrate after the photoirradiation for 0.3 h (100% for Acr$^+$–Mes). The low yield of bromination catalyzed by Me$_2$Acr$^+$–Mes is attributed to the lower quantum yield of the ET state of Me$_2$Acr$^+$–Mes as compared with Me$_2$Acr$^+$ (vide infra). The quantum yield of the ET state was obtained from the fluorescence lifetime measurements and the comparative method by time-resolved laser flash photolysis.[36] The fluorescence decays of Me$_2$Acr$^+$–Mes and Me$_2$AcrH$^+$ are shown in Fig. 7. The lifetimes were determined to be 15 ns for Me$_2$Acr$^+$–Mes and 37 ns for 2,7,10-trimethylacridinium (Me$_2$AcrH$^+$). The fluorescence quantum yields were determined to be 0.21 and 0.50 for Me$_2$Acr$^+$–Mes and Me$_2$AcrH$^+$, respectively. Thus, 60% of fluorescence of Me$_2$AcrH$^+$ was quenched by intramolecular electron transfer from the Mes moiety to the singlet excited state of Me$_2$AcrH$^+$ to form the ET state. The quantum yield of the ET state was directly determined from the transient absorption spectrum of the ET state of Me$_2$Acr$^+$–Mes and the molar absorption coefficient of one-electron reduced Me$_2$Acr$^+$–Mes (Me$_2$Acr$^\bullet$–Mes, $\varepsilon = 5000$ M^{-1} cm^{-1} at 520 nm in MeCN) obtained from electron-transfer reduction of Me$_2$Acr$^+$–Mes with tetramethyl-p-benzosemiquinone radical anion. The quantum yield of the ET state was 60% in MeCN, which is significantly smaller than the value of Acr$^+$–Mes (98%).[20a]

In contrast to the case of Acr$^+$–Mes, the photocatalytic bromination of TMB with O$_2$ in the presence of 9-phenyl-10-methylacridinium ion (Acr$^+$–Ph) proceeds via electron transfer from TMB to the singlet excited state of Acr$^+$–Ph (^{1}Acr$^+$–Ph*). The reactivity was particularly decreased because Acr$^+$–Ph does not have a reducing ability at the photoexcited state. The yield of bromination was 10% with 0.6% quantum yield for 0.3 h photoirradiation. The lifetime of ^{1}Acr$^+$–Ph* ($\tau = 1.5$ ns in MeCN)[37] is much shorter than that of the ET state of Acr$^+$–Mes. A high concentration of substrate is required to quench the short-lived ^{1}Acr$^+$–Ph*.

We have also examined photocatalytic reactions of mesitylene or durene in with Acr$^+$–Mes and HBr in O$_2$-saturated MeCN.
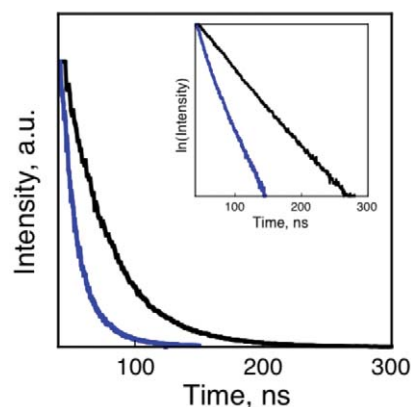
Fig. 7 Fluorescence decay curves of Me$_2$Acr$^+$–Mes (5.0×10^{-5} M, blue) and Me$_2$AcrH$^+$ (5.0×10^{-5} M, black) in deaerated MeCN. Excitation wavelength: 430 nm. Monitoring wavelength: 510 nm. Inset: First-order plots.

The one-electron oxidation of durene and mesitylene with the $Mes^{\bullet+}$ moiety are thermodynamically possible, because the E_{ox} values of the substrates (1.98 V *versus* SCE for mesitylene; 1.63 V for durene)[31] are lower than the E_{red} value of $Mes^{\bullet+}$ (2.06 V).[21] However, no bromination occurred under the present photocatalytic conditions. The deprotonation of the radical cation of toluene derivatives such as mesitylene and durene occurs more efficiently to yield the benzyl radical. This is followed by rapid O_2 addition to afford the peroxyl radical, leading to the corresponding aldehyde.[21] Thus, the main products in photoreaction of mesitylene and durene with HBr in the presence of O_2 for 1.5 h were 3,5-dimethylbenzaldehyde (16% yield) and 2,4,5-trimethylbenzaldehyde (10%), respectively.

Summary

The photocatalytic bromination reaction proceeds *via* intra-molecular photoinduced electron transfer from the Mes moiety to the singlet excited state of the Acr^+ moiety of Acr^+–Mes to generate $Acr^{\bullet}$–$Mes^{\bullet+}$, followed by electron transfer from the substrates to the $Mes^{\bullet+}$ moiety of $Acr^{\bullet}$–$Mes^{\bullet+}$ and also electron transfer from the $Acr^{\bullet}$ moiety to O_2 with H^+ to produce $HO_2^{\bullet}$, accompanied by regeneration of Acr^+–Mes. The resulting substrate radical cation reacts with Br^- to produce the Br adduct radical, which undergoes dehydrogenation with $HO_2^{\bullet}$ to yield the corresponding brominated product and hydrogen peroxide. H_2O_2 reacts with HBr and the substrate to yield another brominated product and H_2O. Thus, the use of Acr^+–Mes as a photocatalyst has enabled us to accomplish the selective photobromination of aromatic hydrocarbons and thiophenes with HBr as a Br source and oxygen as a green oxidant without using a toxic bromine source. Although the substrates that can be brominated are limited by their oxidation potentials, this limitation is compensated for by the high selectivity for the bromination to avoid over-bromination. Such a selective photocatalytic bromination reaction by the present method *via* electron transfer can allow us the large-scale synthesis without the cost of isolation and purification.

Experimental

Materials

Chemicals were purchased from a commercial source and used without further purification, unless otherwise noted. 9-Mesityl-10-methylacridinium perchlorate [(Acr^+–Mes)ClO_4^-], 9-mesityl-2,7,10-trimethylacridinium perchlorate [(Me_2Acr^+–Mes)-ClO_4^-] and 9-phenyl-10-methylacridinium perchlorate [(Acr^+–Ph)ClO_4^-] were commercially obtained from Tokyo Chemical Industry, Japan. Acetonitrile was of spectral grade, obtained commercially and used without further purification.

Reaction procedures and isolation of 2,4,5-trimethoxybromobenzene

The photocatalytic reactions were carried out by the following procedure. Typically, a CD_3CN solution (0.6 mL) containing (Acr^+–Mes)ClO_4^- (0.20 mM) and 1,2,4-trimethoxybenzene (TMB, 4.0 mM) in an NMR tube with a rubber septum was saturated with oxygen by bubbling oxygen through a stainless

steel needle for 5 min before adding HBr (20 mM). The solution was then irradiated with a 500 W xenon lamp (Ushio Optical ModelX SX-UID 500XAMQ) through a color glass filter that cuts off light of $\lambda < 320$ nm at 298 K. After photoirradiation, the corresponding brominated product was identified and quantified by comparison of the ^1H NMR spectra with that of an authentic sample and an internal standard. The chemical shifts of all products are listed in ESI S2.†

A brominated product, 2,4,5-trimethoxybromobenzene was isolated by the following procedure. Typically, (Acr^+–Mes)ClO_4^- (18 mg, 0.044 mmol) and TMB (0.2 g, 1.2 mmol) were dissolved in an MeCN solution (100 mL) containing 50% aqueous HBr (160 μL, 1.5 mmol). The solution was stirred under photoirradiation through the glass of an aqueous solution of copper sulfate as a color filter ($\lambda = 320$–600 nm) at 298 K for 24 h. The reaction mixture was neutralized by adding aqueous NaOH, then diluted with hexane (100 mL) and distilled water (100 mL). The organic layer was washed three times with water (50 mL × 3) and then dried using Na_2SO_4. The isolated yield of 2,4,5-trimethoxybromobenzene was 61% (0.18 g, 0.73 mmol).

GC-mass measurements

GC-mass measurements were carried out with a Shimadzu GC-17A gas chromatograph and QP5000 mass spectrometer (electron ionization method) which was equipped with a flame ionization detector and a capillary column (122–5532, DB-5MS), 30 m × 0.25 mm. Helium was used as a carrier gas.

Quantum yield determinations

A standard actinometer (potassium ferrioxalate)[38] was used for the quantum yield determination of the photocatalytic bromination of organic substrates with HBr in the presence of Acr^+–Mes in O_2-saturated MeCN. Typically, a square quartz cuvette (10 mm i.d.), which contained a deaerated CH_3CN solution (3.0 cm³) of Acr^+–Mes (2.0×10^{-4} M) and 1,2,4-trimethoxybenzene, was irradiated with monochromatic light of $\lambda = 430$ nm from a Shimadzu RF-5300PC fluorescence spectrophotometer. Under the conditions of actinometry experiments, the actinometer and Acr^+–Mes absorbed essentially all incident light of $\lambda = 430$ nm. The light intensity of monochromatized light of $\lambda = 430$ nm was determined to be 2.7×10^{-8} einstein s^{-1}. The quantum yields were determined by gas chromatography and ^1H NMR spectroscopy from increases in the GC and ^1H NMR peaks due to the corresponding aromatic bromide.

Electrochemical measurements

Second harmonic ac voltammetry (SHACV)[39,40] measurement of aromatic substrates were carried out with ALS630B electrochemical analyzers in deaerated MeCN containing 0.20 M $Bu_4N^+ClO_4^-$ (TBAP) as a supporting electrolyte at 298 K. The carbon working electrode (BAS, surface i.d. 1.6 mm) was polished with BAS polishing alumina suspension and rinsed with acetone before use. The counter electrode was a platinum wire. The measured potentials were recorded with respect to an Ag/AgNO$_3$ (0.01 M) reference electrode. The E_{ox} values (*versus* Ag/AgNO$_3$) are converted into those *versus* SCE by addition of 0.29 V.[41]

Laser flash photolysis measurements

Measurements of transient absorption spectra in the photo-chemical reaction of Acr^+–Mes with aromatic substrates and/or aqueous HBr were performed according to the following procedure. Typically, an MeCN solution containing Acr^+–Mes (1.0×10^{-4} M) and 1,2,4-trimethoxybenzene (1.0×10^{-3} M) was excited by Nd : YAG laser (continuum, SLII-10, 4–6 ns FWHM) at 430 nm. Time dependence of the transient absorption spectra were measured by using a continuous Xe-lamp (150 W) and an In GaAs-PIN photodiode (Hamamatsu 2949) as a probe light and a detector, respectively. The output from the photodiodes and a photomultiplier tube was recorded with a digitizing oscillo-scope (Tektronix, TDS3032, 300 MHz). All experiments were performed at 298 K.

Time-resolved fluorescence decay measurements

The fluorescence lifetimes of Me_2Acr^+–Mes and Me_2AcrH^+ were measured by a Photon Technology International GL-3300 with a Photon Technology International GL-302, nitrogen laser/pumped dye laser system, equipped with a four channel digital delay/pulse generator (Stanford Research System Inc. DG535) and a motor driver (Photon Technology International MD-5020). Excitation wavelength was 430 nm using a toluene solution con-taining dimethyl-POPOP [1,4-bis(4-methyl-5-phenyl-2-oxazolyl) benzene] (Dojindo, Japan) as a laser dye.

Theoretical calculations

Density functional theory (DFT)[42] calculations were performed with Gaussian03 (Revision C.02, Gaussian, Inc.).[43] The calcu-lations were performed on a 32-processor QuantumCube™ at the B3LYP/6-31G(d) and B3LYP/6-31+G(d,p) level of theory. Graphical outputs of the computational results were generated with the *GaussView* software program (ver. 3.09) developed by Semichem, Inc.[44]

Acknowledgements

Notes and references

1 (a) *March's Advanced Organic Chemistry: Reactions, Mechanisms, and Structure*, 6th ed., ed. M. B. Smith and J. March, Wiley, New York, 2007, pp. 698–705; (b) *Comprehensive Organic Transformations*, 2nd ed., ed. R. C. Larock, Wiley-VCH, New York, 1999, pp. 622–624.
2 (a) B. Das, K. Venkateswarlu, M. Krishnaiah and H. Holla, *Tetrahedron Lett.*, 2006, **47**, 8693; (b) B. Das, K. Venkateswarlu, A. Majhi, V. Siddaiah and K. R. Reddy, *J. Mol. Catal. A: Chem.*, 2007, **267**, 30.
3 A. Podgorsek, M. Zupan and J. Iskra, *Angew. Chem., Int. Ed.*, 2009, **48**, 8450.
4 A. Molinari, G. Varani, E. Polo, S. Vaccari and A. Maldotti, *J. Mol. Catal. A: Chem.*, 2007, **262**, 156.
5 G. K. S. Prakash, T. Mathew, D. Hoole, P. M. Esteves, Q. Wang, G. Rasul and G. A. Olah, *J. Am. Chem. Soc.*, 2004, **126**, 15770.
6 F. Kakiuchi, T. Kochi, H. Mutsutani, N. Kobayashi, S. Urano, M. Sato, S. Nishiyama and T. Tanabe, *J. Am. Chem. Soc.*, 2009, **131**, 11310.
7 G. A. Olah, T. Mathew, E. R. Marinez, P. M. Esteves, M. Etzkorn, G. Rasul and G. K. S. Prakash, *J. Am. Chem. Soc.*, 2001, **123**, 11556.
8 A. Messerschmidt and R. Wever, *Proc. Natl. Acad. Sci. U. S. A.*, 1996, **93**, 392.
9 (a) K. Kikushima, T. Moriuchi and T. Hirao, *Chem.–Asia. J.*, 2009, **4**, 1213; (b) T. Moriuchi, M. Yamaguchi, K. Kikushima and T. Hirao, *Tetrahedron Lett.*, 2007, **48**, 2667.
10 V. Nair, S. B. Panicker, A. Augustine, T. G. George, S. Thomas and M. Vairamani, *Tetrahedron*, 2001, **57**, 7417.
11 L. C. Blasiak and C. L. Drennan, *Acc. Chem. Res.*, 2009, **42**, 147.
12 K. G. Dewkar, V. S. Narina and A. Sudalai, *Org. Lett.*, 2003, **5**, 4501.
13 (a) C. Ye and M. J. Shreeve, *J. Org. Chem.*, 2004, **69**, 8561; (b) V. A. Joshi, M. Baidossi, Mulhopadhyay and Y. Sasson, *Org. Process Res. Dev.*, 2004, **8**, 568.
14 P. K. Chhattise, A. V. Ramaswamy and S. B. Waghmode, *Tetrahedron Lett.*, 2008, **49**, 189.
15 L. C. Blasiak and C. L. Drennan, *Acc. Chem. Res.*, 2009, **42**, 147.
16 (a) E. Baciocchi, C. Crescenzi and O. Lanzalunga, *Tetrahedron*, 1997, **53**, 4469; (b) J. Eriksen, C. S. Foote and T. L. Parker, *J. Am. Chem. Soc.*, 1977, **99**, 6455; (c) N. Soggiu, H. Cardy, J. L. Habib and J. P. Soumillon, *J. Photochem. Photobiol., A*, 1999, **124**, 1; (d) E. Baciocchi, T. Del Giacco, F. Elisei, M. F. Gerini, M. Guerra, A. Lapi and P. Liberali, *J. Am. Chem. Soc.*, 2003, **125**, 16444; (e) Y. Che, W. Ma, Y. Ren, C. Chen, X. Zhang, J. Zhao and L. Zang, *J. Phys. Chem. B*, 2005, **109**, 8270; (f) S. Lacombe, H. Cardy, M. Simon, A. Khoukh, J. P. Soumillon and M. Ayadim, *Photochem. Photobiol. Sci.*, 2002, **1**, 347; (g) T. Pigot, T. Arbitre, M. Hervé and T. S. Lacombe, *Tetrahedron Lett.*, 2004, **45**, 4047; (h) V. Latour, T. Pigot, M. Simon, H. Cardy and S. Lacombe, *Photochem. Photobiol. Sci.*, 2005, **4**, 221.
17 S. M. Bonesi, I. Manet, M. Freccero, M. Fagnoni and A. Albini, *Chem.–Eur. J.*, 2006, **12**, 4844.
18 N. L. Bauld, in *Advances in Electron Transfer Chemistry*, ed. P. S. Mariano, JAI Press, Greenwich, CT, 1992, vol. 2, pp. 1–66.
19 (a) F. Müller and J. Mattay, *Chem. Rev.*, 1993, **93**, 99; (b) M. Schmittel and A. Burghart, *Angew. Chem., Int. Ed. Engl.*, 1997, **36**, 2550; (c) V. Dichiarante, M. Fagnoni, M. Mella and A. Albini, *Chem.–Eur. J.*, 2006, **12**, 3905; (d) E. Baciocci, M. Bietti and O. Lanzalunga, *Acc. Chem. Res.*, 2000, **33**, 243; (e) T. Herberts, F. Blume and H. D. Roth, *J. Am. Chem. Soc.*, 1998, **120**, 4591.
20 (a) S. Fukuzumi, K. Kotani, K. Ohkubo, S. Ogo, N. V. Tkachenko and H. Lemmetyinen, *J. Am. Chem. Soc.*, 2004, **126**, 1600; (b) K. Ohkubo, H. Kotani and S. Fukuzumi, *Chem. Commun.*, 2005, 4520.
21 K. Ohkubo, K. Mizushima, R. Iwata, K. Souma, N. Suzuki and S. Fukuzumi, *Chem. Commun.*, 2010, **46**, 601.
22 (a) H. Kotani, K. Ohkubo and S. Fukuzumi, *J. Am. Chem. Soc.*, 2004, **126**, 15999; (b) K. Ohkubo and S. Fukuzumi, *Bull. Chem. Soc. Jpn.*, 2009, **82**, 303; (c) K. Ohkubo, R. Iwata, T. Yanagimoto and S. Fukuzumi, *Chem. Commun.*, 2007, 3139; (d) K. Ohkubo, T. Nanjo and S. Fukuzumi, *Catal. Today*, 2006, **117**, 356; (e) K. Ohkubo, K. Yukimoto and S. Fukuzumi, *Chem. Commun.*, 2006, 2504; (f) K. Ohkubo, R. Iwata, S. Miyazaki, T. Kojima and S. Fukuzumi, *Org. Lett.*, 2006, **8**, 6079.
23 K. T. Potts, M. J. Cipullo, P. Ralli and G. Theodoridis, *J. Org. Chem.*, 1982, **47**, 3027.
24 (a) P. Arsenyan, E. Paegle and S. Belyakov, *Tetrahedron Lett.*, 2010, **51**, 205; (b) P. Arsenyan, O. Pudova, J. Popelis and E. Lukevics, *Tetrahedron Lett.*, 2004, **45**, 3109.
25 T. J. Dingemans, N. S. Murthy and E. T. Samulski, *J. Phys. Chem. B*, 2001, **105**, 8845.
26 M. M. Murray, P. Kaszynski, D. A. Kaisaki, W. Chang and D. A. Dougherty, *J. Am. Chem. Soc.*, 1994, **116**, 8152.
27 (a) S. Fukuzumi, H. Kotani and K. Ohkubo, *Phys. Chem. Chem. Phys.*, 2008, **10**, 5159; (b) S. Fukuzumi, R. Hanazaki, H. Kotani and K. Ohkubo, *J. Am. Chem. Soc.*, 2010, **132**, 11002.
28 For formation of π-dimer radical cations of aromatic compounds with near-IR absorption bands, see: (a) J. K. Kochi, R. Rathore and P. Le Maguerus, *J. Org. Chem.*, 2000, **65**, 6826; (b) S. V. Rosokha, M. D. Newton, A. S. Jalilov and J. K. Kochi,

J. Am. Chem. Soc., 2008, **130**, 1944; (*c*) D. Small, V. Zaitsev, Y. Jung, S. V. Rosokha, M. Head-Gordon and J. K. Kochi, *J. Am. Chem. Soc.*, 2004, **126**, 13850.

29 P. K. Das and K. Borowski, *J. Chem. Soc., Faraday Trans. 2*, 1981, **77**, 1009.

30 In the presence of 20 mM HBr, no transient absorption spectrum was observed because all of the photoinduced events were completed in microseconds which is time-resolved limitation for our nanosecond laser flash system.

31 S. Fukuzumi, K. Ohkubo, T. Suenobu, K. Kato, M. Fujitsuka and O. Ito, *J. Am. Chem. Soc.*, 2001, **123**, 8459.

32 D. T. Sawyer, T. S. Calderwood, K. Yamaguchi and C. T. Angelis, *Inorg. Chem.*, 1983, **22**, 2577.

33 No H_2O_2 was observed after the photocatalytic reaction as checked by iodometric titration and ^1H NMR spectroscopy.

34 A. Podgorsek, S. Stavber, M. Zupan and J. Iskra, *Tetrahedron*, 2009, **65**, 4429.

35 P. B. Markel, P. L. Joseph, J. P. Dinnocenzo and S. Farid, *J. Org. Chem.*, 2009, **74**, 5163.

36 K. Ohkubo, H. Kotani, J. Shao, Z. Ou, K. M. Kadish, G. Li, R. K. Pandey, M. Fujitsuka, O. Ito, H. Imahori and S. Fukuzumi, *Angew. Chem., Int. Ed.*, 2004, **43**, 853.

37 K. Ohkubo, K. Suga, K. Morikawa and S. Fukuzumi, *J. Am. Chem. Soc.*, 2003, **125**, 12850.

38 C. G. Hatchard and C. A. Parker, *Proc. R. Soc. London, Ser. A*, 1956, **235**, 518.

39 *Electrochemical Methods, Fundamental and Applications*, ed. A. J. Bard and L. R. Faulkner, John Wiley & Sons, New York, 2001, chap. 10, pp. 368–416.

40 The SHACV method provides a superior approach to directly evaluating the one-electron redox potentials in the presence of a follow-up chemical reaction, relative to the better-known dc and fundamental harmonic ac methods (*a*) A. M. Bond and D. E. Smith, *Anal. Chem.*, 1974, **46**, 1946; (*b*) E. M. Arnett, K. Amarnath, N. G. Harvey and J.-P. Cheng, *J. Am. Chem. Soc.*, 1990, **112**, 344.

41 *Electrochemical Reactions in Non-aqueous Systems*, ed. C. K. Mann and K. K. Barnes, Mercel Dekker, New York, 1970.

42 (*a*) A. D. Becke, *J. Chem. Phys.*, 1993, **98**, 5648; (*b*) C. Lee, W. Yang and R. G. Parr, *Phys. Rev. B: Condens. Matter*, 1988, **37**, 785; (*c*) W. J. Hehre, L. Radom, P. v. R. Schleyer and J. A. Pople, *Ab Initio Molecular Orbital Theory*, Wiley, New York, 1986.

43 *Gaussian 03*, M. J. Frisch, G. W. Trucks, H. B. Schlegel, G. E. Scuseria, M. A. Robb, J. R. Cheeseman, V. G. Zakrzewski, J. A. Montgomery, R. E. Stratmann, J. C. Burant, S. Dapprich, J. M. Millam, A. D. Daniels, K. N. Kudin, M. C. Strain, O. Farkas, J. Tomasi, V. Barone, M. Cossi, R. Cammi, B. Mennucci, C. Pomelli, C. Adamo, S. Clifford, J. Ochterski, G. A. Petersson, P. Y. Ayala, Q. Cui, K. Morokuma, D. K. Malick, A. D. Rabuck, K. Raghavachari, J. B. Foresman, J. Cioslowski, J. V. Ortiz, B. B. Stefanov, G. Liu, A. Liashenko, P. Piskorz, I. Komaromi, R. Gomperts, R. L. Martin, D. J. Fox, T. Keith, M. A. Al-Laham, C. Y. Peng, A. Nanayakkara, C. Gonzalez, M. Challacombe, P. M. W. Gill, B. G. Johnson, W. Chen, M. W. Wong, J. L. Andres, M. Head-Gordon, E. S. Replogle and J. A. Pople, Gaussian, Inc., Pittsburgh, PA, 2003.

44 R. Dennington II, T. Keith, J. Millam, K. Eppinnett, W. L. Hovell and R. Gilliland, Semichem, Inc., Shawnee Mission, KS, 2003.